Proceedings of the 7th International Symposium on Cavitation
CAV2009 – Paper No. 149
August 17-22, 2009, Ann Arbor, Michigan, USA

Mechanism and Scalability of Tip Vortex Cavitation Suppression by Water and Polymer Injection

Natasha A. Chang
University of Michigan
Ann Arbor, MI, USA

Ryo Yakushiji
University of Michigan
Ann Arbor, MI, USA

Harish Ganesh
University of Michigan
Ann Arbor, MI, USA

Steven L. Ceccio
University of Michigan
Ann Arbor, MI, USA

ABSTRACT

Tip Vortex Cavitation (TVC) suppression via mass injection in the core of the vortex was studied with an elliptical plan-form hydrofoil NACA-66 modified in a re-circulating water tunnel with known nuclei distribution. The chord base Reynolds number was O(10^6) for all the experiments. The injectants were water and Polyox WSR-301 solutions with concentration ranging from 10 to 500 *wppm*. Flow rates of $0.033 < Q_{jet} / Q_{core} < 0.27$ were examined. It was found that the TVC suppression effect was more pronounced for inception than for desinence. For inception, a suppression effect was observed for all cases of mass injection. The baseline *inception* cavitation number, σ_I = 3.3, was higher than the average minimum pressure coefficient, $-Cp$ = 2.3 inferred from the average vortex flow properties near the location of TVC inception. Injection of mass into the core reduced the observed inception cavitation number to a value that was consistent with the average value such that $\sigma_I \sim \sigma_D \sim -Cp$. The measured TVC *desinence* value for the baseline case was found to match the expected minimum $-Cp$. The effect on polymer injection on TVC desinence was twice as strong as that for water injection. The mechanisms that lead to TVC suppression *via* mass injection are also discussed.

INTRODUCTION

Tip vortex cavitation (TVC) the inception and development that is associated with lifting surface has been extensively studied due to their importance in the design of turbo-machinery and propulsors (Arndt, 2002). The flow fields and resulting TVC has been studied on elliptic planform hydrofoils by numerous researchers, including Fruman *et al*. (1991), Fruman *et al.* (1992), and Arndt and Maines (1994) and (2000). These studies reveled the importance of both the detailed flow around the hydrofoil tip and the ambient nuclei distribution to the process of TCV inception.

A number of methods have been developed to delay the onset of TVC. The strategies used can be classified into passive and active methods. A survey of several different strategies is presented by Platzer and Souders (1979). Examples of passive methods are hydrofoil surface treatments and tip treatments (*e.g.* bulb, winglets). Generally suppression is achieved through the increase of the vortex core radius (Platzer and Souders 1979, Souders and Platzer 1981). Active cavitation control can be achieved through mass injection into the core of the vortex (Platzer and Souders 1979, Souders and Platzer 1981). This form of cavitation suppression is the object of study for this effort.

In the study conducted by Souders and Platzer (1981), water at 40% Dissolved Oxygen taken from the test facility was injected back into the tip flow. An elliptic foil with a modified NACA 66 section was used in flows with Reynolds numbers order of 10^6. Souders and Platzer (1981) defined cavitation inception as the first appearance of cavitation, generally observed at one chord-length downstream from the foil as the free stream pressure was reduced. They observed that mass injection near the tip region delayed the onset of cavitation reducing the incipient cavitation number by as much as 40%.

Injection of high-molecular weight polymer solutions have also been shown to have a cavitation suppression effect (Ting 1974). In the subsequent studies of TVC suppression, active and passive injection of a mass included the use of polymer solutions. Fruman and Afalo (1989) and Fruman *et al* (1995) studied TVC suppression by using elliptical plan-form hydrofoils at Reynolds number of order 10^5 to 10^6. They examined injection 500 *wppm* and 1000 *wppm* solutions of Polyox WSR-301, water, and a water-glycerin mix. Cavitation densinense was used as a measure of TVC suppression. It was found that there was no significant gain in TVC suppression when injecting water or water-glycerin mix. The injection of a polymer solution, however, did provide a reduction of at least 25% in the inception cavitation number. Laser Doppler Velocimetry measurements were conducted at 0.125, 0.25, 0.5 and 1 chord length from the tip of the foil. It was observed that water or water-glycerin injection modified the axial component of the flow in the core of the vortex, producing a net deficit, but the tangential component remained unchanged. In polymer injection the axial component of the core velocity changed in a similar fashion that observed for to water and water-glycerin injection. The maximum tangential component of the velocity

was found to decrease, and the core radius was found to increase; hence, injection affected the process of vortex roll-up. However, the coefficient of lift did not change, so the overall vortex strength remained the same. Moreover, it was observed that the root mean square (RMS) of the axial velocity decreased for the cases where mass was being injected to the core.

The authors stated that the two effects could be at work that would reduce the inception index. First, injection can lead to an increase in core radius and a decrease in the maximum tangential velocity, could lead to an increase in the core pressure, and cavitation desinence delay. Second, the modified rheology of the tip flow (in the case of polymer injection) can lead to suppression. The flow disruption from jet swelling of a viscoelastic injectant was also conjectured to cause TVC suppression (Fruman and Galivel 1980). However, it is not thought that the presence of the polymer significantly alters the bubble dynamics during inception (Chahine and Fruman 1979).

The mass injection effect on TVC suppression was also studied using a scaled five-blade-propeller by Chahine *et al.* (1993). Cavitation desinence was used as the measure for TVC. They found that the TVC suppression was not significant with injection of water and water-glycerin injections, but a significant delay in the onset of cavitation could be observed when a solution of Polyox WSR-301 was injected at 1000 *wppm* to 7000 *wppm*. They reported found that the injection port location was crucial; the mass had to be injected into the core of the vortex for the maximum suppression effect to take place. The authors suggested that injection of the polymer modifies the tangential velocity profile of the tip vortex, leading to an increase the core pressure.

In summary, researchers that used cavitation *inception* or the first appearance of cavitation, as the measure for TVC observed that cavitation was suppressed by injection of a mass into the core of the vortex. Conversely, investigators that used cavitation *desinence* or the disappearance of well developed TVC, as the measurable for TVC only observed a suppression effect if polymer solutions were injected. The measured cavitation desinence correlated well with the negative of the estimated pressure coefficient for the tip vortex based on the measured mean tangential velocity profile.

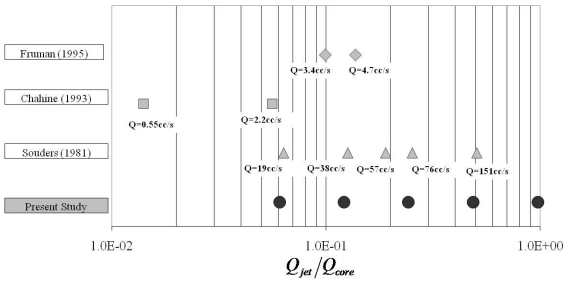

Table 1: Summary of the previous test conditions and the test conditions explored in this effort for the study of TVC suppression. Q_{jet} is the volume flux rate of the injected solution, and Q_{core} is defined as the volume flux rate of the underlying flow field through the vortex core, which was estimated from flow field measurements described in results section.

The objective of the current effort is to systematically study the TVC suppression effect on an elliptical plan-form hydrofoil from the injection of both water and Polyox WSR-301. Table 1 presents a summary of previously reported injection conditions along with those of the present study. The parameter range selected also attempts to capture the relationship between the injected volumetric flux, the polymer concentration, and the TVC suppression observed. Therefore, the range of volumetric flux and concentration was chosen from near zero values, to values where the TVC suppression effect appeared saturated.

EXPERIMENTAL SET UP

Flow Facilities and Test Models

The experiments were conducted in the University of Michigan 9-Inch Water Tunnel. Upstream of the test section the water tunnel has a series of flow management screens followed by a circular contraction with an area ratio of 6.4:1. The test section has a 0.229 *m*, or approximately 9-inch, diameter inlet that smoothly transitions to a 0.22 *m* by 0.22 *m* rounded rectangular cross section. The length of the test section is 1 *m*. The test section has four acrylic windows that are 0.939 *m* by 0.100 *m* for viewing purposes. The flow speed and static pressure in the test section can be controlled to values between 0 to 18 *m/s* and from near vacuum to 200 *kPa*. A de-aeration system is used to control the dissolved oxygen content of the water. The including the de-aeration system the tunnel holds 3.8 m^3 of water, which is filtered at the inlet to 1 micron. The water tunnel itself holds 3.2 m^3 of water.

The hydrofoil used had an elliptic planform with a NACA66 section following the modifications reported by Souder and Platzer (1981). The chord to half-span ratio is 1, and the maximum ratio of hydrofoil thickness to chord is 0.099. The chord length was 0.114 *m*. Aqueous solutions were injected through the hydrofoil in a tube of 2.36 *mm* in diameter. As the flow reached the tip of the hydrofoil the tube diameter reduces to 1.59 *mm*, matching the injection nozzle of the aqueous solution. The surface of the suction side 6 *mm* from the leading edge of the hydrofoil was roughened by gluing Aluminum Dioxide particles to the surface. A schematic is shown in Figure 1.

The hydrofoil was mounted on the top window of the water tunnel test section. The angle of attack, α, could be varied, and it was set to 8 +/- 0.1 degrees. The water was de-aerated to achieve between 20% and 30% Dissolved Oxygen (DO) content at atmospheric pressure, which was measured with a Thermo Scientific Orion 3 Star meter equipped with a 081010MD probe. The water and aqueous polymer solutions were injected using a constant volume pump (Figure 2). The flow velocity in the tunnel test section, U_∞, was set to 8 +/- 0.3 *m/s* and 10 +/- 0.3 *m/s* yielding a chord-based Reynolds number of 0.91 x 10^6 and 1.13 x 10^6.

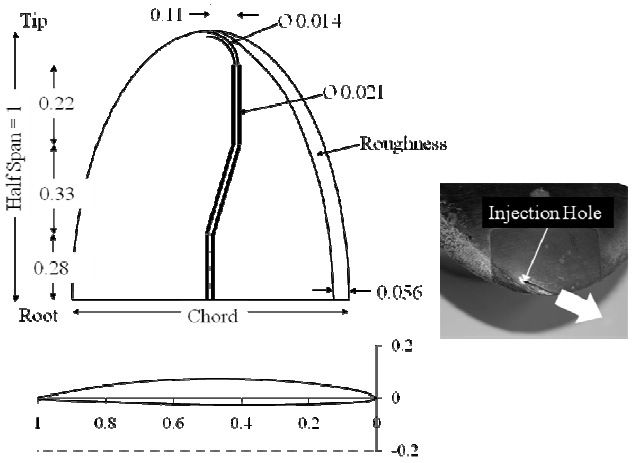

Figure 1: Elliptic plan-form foil NACA66 (DTNSRDC modified) with a chord length of 114.3 *mm*, half–span of 114.3 *mm*, and a maximum ratio of the thickness to chord of 0.099. All measurements are given in non-dimensional form with respect to the chord length, c = 0.114 *m*.

The free-stream static pressure, P_∞, ranged from 60 to 195 *kPa*. This corresponds to a free-stream cavitation number, σ_∞, ranging from 1.7 to 4.8, where P_V is the water vapor pressure and ρ is the water density:

$$\sigma_\infty = \frac{P_\infty - P_V}{\frac{1}{2}\rho U_\infty^2} \qquad (1)$$

Injected Water and Polymer Solution

The polymer used was poly(ethylene oxide) (PEO) with mean molecular weight of 4 million, Polyox WSR-301. The polymer solution was prepared with de-aerated water from the water tunnel with DO of 25%. The chlorine in the water was neutralized to prevent polymer degradation by adding 0.1 g/liter of Sodium Thiosulfate. The water was weighed with an Acculab SV-30 scale with an error of +/- 0.005 *kg*, and the polymer was weighed with an Acculab VIC-212 scale with an error of +/- 0.01g. The polymer resin granules were then slowly added to the water while it was being stirred. To fully hydrate the polymer in the water the solution was covered and allowed to sit for 48 hrs. The base polymer solution was prepared at 2000 *wppm*, this was then diluted 2 hours prior to testing to the test concentrations which ranged from 10 *wppm* to 500 *wppm* with de-aerated water from the tunnel collected 24 hours prior at DO of 25%. The polymer solution preparation was accurate to +/- 3% of the final concentration achieved.

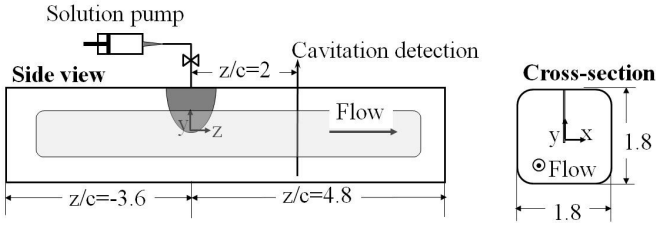

Figure 2: Experimental set-up in the water tunnel test section of the hydrofoil and aqueous solution injection system. All measurements are given in non-dimensional form with respect to the chord length c = 0.114 *m*.

The DO of the fluid being injected was measured prior to testing. The DO was maintained between 60% and 90% to ensure that any suppression effect observed would be due to changes in the flow and not due to the addition of injectant with fewer nuclei than the free-stream fluid. Super-saturated water (directly from the house water supply) was not used because it created visible air bubbles in the injection system.

Mass Injection and Polymer Solution Degradation

The water or polymer solution was injected *via* two methods depending on the mass flow rate required. For mass flow rates less than 8 *cc/s*, a syringe pump was used. The pump consisted of a pair of large syringes that had an outlet port of 7.9 *mm* inner diameter. When in operations all valves (total of two) from the pump leading to the hydrofoil are fully open to prevent polymer degradation. This syringe system is the same as that used in Yakushiji *et al.* (2008).

For higher flow rates up to a maximum of 28.2 *cc/s* gas pressure was used to inject the fluid. The fluid was placed in a pressurized tank with an exit port having an inner diameter of 7.9 *mm* inches. There was only one valve between the vessel and the hydrofoil that was fully open when injecting mass. The flow rate was established while the water tunnel was under test flow conditions by measuring the mass loss of the tank before and after injection. The necessary driving pressure for the vessel was established for a given free-stream static pressure, and the pressure in the vessel was regulated with an Omega PRG101-120 from the house compressed air supply. The accuracy and repeatability of injectant flow rate was established by setting a given flow rate 4 different times for a given flow and pressure condition. As the free-stream static pressure of the water tunnel was changed the pressure in the vessel was changed accordingly and the mass flow rate measured. It was found that for flow rates between 10 and 20 *cc/s* the accuracy is +/- 1 *cc/s*. For higher flow rates 20 *cc/s* and above the accuracy was +/- 0.5 *cc/s*.

Fruman and Aflalo (1989) conducted a TVC suppression test with a hydrofoil in a homogenous 10 *wppm* polymer solution and found that the cavitation inception was suppressed by 15% due to a reduction of overall hydrofoil lift (resulting in a weaker tip vortex). The tests in this effort were conducted such that the background polymer build up in the water tunnel was maintained below 1 *wppm*, and well below 10 *wppm*, where the polymer build up is expected to significantly affect the hydrofoil lift. The polymer build up was estimated by measuring the amount of fluid injected and diluting it in 1000 gallons of water contained in the tunnel. In addition the background chlorine of the water in the tunnel was periodically measured with an Extech Instrument Extik CL200. The presence of a low level of chlorine, which reacts with the polymer, indicated that the polymer build up was less than 1 *wppm*.

PEO degrades easily when subjected to high levels of shear. Winkel *et al.* (2008) report a criterion for which the polymer will shear and degrade:

$$\gamma = \frac{Q_{jet}}{2\pi r_{nozzle}^3} < 10{,}000\ 1/s \qquad (2)$$

The highest flow rate was 28.2 *cc/s*, which corresponds to a shear rate, $\gamma =$ 8766 1/*s*. Higher flow rates were avoided in order to avoid polymer degradation during as the polymer was injected. In addition, the number of valves and the size of the pipes were similar to Yakushiji *et al.* (2008). The level of polymer degradation was measured using a similar experimental method described in Virk (1970). Samples were prepared, injected, and collected at the hydrofoil injector exit. The collected samples were then diluted. Then, the samples were flowed through a lone pipe, and the resulting pressure drop was recorded as a function of flow rate. The level of drag reduction thus determined was compared to a non-injected sample of the same concentration to determine if injection had led to significant polymer degradation. For the given experimental set up no degradation was observed (Yakushiji *et al.*, 2008), therefore none was expected in the experiments conducted in this work.

The flux of the injected liquid was scaled with the nominal flux of liquid in the core of the tip vortex, $Q_{\text{core}} = \pi r_{\text{core}}^2 U_\infty$, where the core radius was determined through flow visualization (discussed below). The experimental conditions studied are listed in Table 2. The different injection rates and polymer solution concentration were studied at a variety of pressures, from no cavitation to fully cavitating. For a given injection rate and polymer solution the free-stream flow velocity was set and the pressure was varied. This ensured that relative cavitation number within a data set was accurate to +/- 0.02 given that the pressure could be set to +/-1 *kPa*, and the temperature varied less than 10 degrees Celsius between the beginning and the end of the experiment. The cavitation measurements were taken for a baseline flow with a free-stream velocity, $U_\infty = 10$ *m/s*.

Cavitation Detection and Visualization

Cinemagraphic recording of the TVC were recorded using a Phantom V9 high-speed video camera equipped with a 50 *mm* focal length Nikon lens. The camera viewing area was 1632 pixels x 400 pixels, corresponding to a 222 *mm* by 55 *mm* field of view. The furthest downstream location visualized was 1.6 chord-lengths from the tip of the foil imaging the suction side of the hydrofoil.

U_{jet} / U_∞	0.17	0.35	0.70	1.41
Q_{jet} / Q_{core}	0.033	0.066	0.13	0.27
Q_{jet} / C (*wppm*)	3.5 *cc/s*	7.0 *cc/s*	14.1 *cc/s*	28.2 *cc/s*
0	0	0	0	0
15.5				4
31			4	
62		4		16
125	4		16	
250		16		
500	16			

Table 2: Cavitation measurement flow conditions for $U_\infty = 10$ *m/s*. U_{jet} is the mean velocity of the injected mass. Q_{core} is the estimated volumetric flow of the core of the vortex assuming that its mean axial velocity is 10 *m/s*.

The viewing area was illuminated with an Arri Arrilux 200 HMI light source perpendicular to the camera and aimed at the tip of the foil. Cavitation inception measurements visualized at 3000 *fps*. For a free-stream velocity of U_∞, of 10 *m/s*, this corresponds to a downstream displacement of 3.3 *mm* (0.03 chord-lengths) between frames of a bubble moving with the flow. The camera could store a maximum of 0.8 seconds of video data per trigger.

The cavitation inception rate ranged from 1 per second to continuous cavitation in the vortex. Therefore, an acoustic system was used to trigger the camera. A Reson TC-4013 hydrophone, with a receiving sensitivity of -211 +/- 3 *dB* re 1*V/μPa* and 3-*dB* bandwidth from 1 *Hz* to 170 *kHz*, was placed 13 cm away from the foil tip on the side window. It resided in a water pocket in the window, and separated from the flow by 1 cm of acrylic. The signal from the hydrophone was conditioned with a Reson VP-2000 voltage preamplifier with a pass-band of 100 *Hz* to 1 *MHz* and a gain of 10 *dB*. The signal from each preamplifier was further band-pass filtered between 1 *kHz* and 200 *kHz* and amplified with a gain of 40 *dB* with a Khron-Hite 3364 four-pole tunable active filter. Here the filter type was Butterworth and the attenuation was 24 *dB/octave*. The amplified and bandpass-filtered signal was then conditioned with a Stanford Research DG535 Four Channel Digital Delay/Pulse Generator to create a TTL signal to trigger the camera. The voltage required for triggering was generally 0.5 volts, except in poor signal-to-noise (SNR) condition from background tunnel cavitation where it was set 1 volt. For each triggered data set there was typically more than one bubble.

The acquired high-speed video was then reviewed and the streamwise inception location of each bubble with respect to the foil tip was estimated by measuring the distance between the foil-tip to the bubble leading extent. The measured pixel distance was converted *via* a calibration conducted by imaging a ruler in the location of the vortex path under the same optical set up.

There are several different ways to determine cavitation inception or desinence. Previous researchers have primarily evaluated cavitation inception and desinence by visual observations (Arndt and Keller 1992; Fruman *et al* 1989, 1991, 1992, 1995; Chahine *et al* 1993). Desinence has often been used to characterize the cavitating flows since the desinence value is less influenced by the water quality and provides a more conservative estimate of the inception pressure. Furthermore, as the water quality becomes stronger, the difference between the cavitation inception number and desinence number becomes smaller (Arndt and Keller 1992; Fruman *et al.* 1989, 1991, 1992; Gindroz and Billet 1993). Gindroz and Billet (1993) used an acoustic based methods to estimate cavitation inception or desinence, but recent studies have shown that cavitation bubbles can generate varying degrees of noise during their inception, growth, and collapse (Chang *et al.* 2007, Choi and Ceccio 2007) adding uncertainty to this method. Visual observation of cavitation inception can provide a definitive measure of bubble event rates, but it is sometimes limited by the investigator's ability to image the smallest or short-lived cavitation bubbles.

In the present investigation, the cinemagraphic recordings of TVC were used to determine the TVC event rates and

inception and desinence. The overall size of the bubbles relative to the viewing area was used as a measure instead of the commonly used individual bubble count. As cavitation number decreases typically the cavitation bubbles become larger and the number of individual bubbles decreases. Therefore, a more consistent measure from very low event rate (0.5 *Hz*) to fully cavitating vortex core is the ratio of the sum of bubbles length to the length of the viewed vortex core. To conduct the cavitation inception to desinence experiments, the high-speed video camera was set to the same viewing area described for cavitation localization, though the frame rate was set to 65 *fps*, and 10 *s* long videos were acquired. Each frame was then processed with MATLAB, and the relative length of the bubble to the streamwise length of the vortex (in this case 1.6 chord-lengths) that can be view was estimated, B_{ratio}.

For the cavitation localization study the data collected was primarily at the first indication of cavitation 1 to 10 events per second. The cavitation desinence and inception study data was collected at cavitation numbers that span from no measured cavitation in 10 seconds to a fully cavitating vortex. The free-stream static pressure, P_∞, was varied from 85*kPa*to 195*kPa*at 5*kPa*increments (0.1 cavitation number). The spacing between the datum points was such that the cavitation number corresponding to a B_{ratio} of 0.01 (cavitation inception) and 0.9 (cavitation desinence) can be estimated via linear interpolation to +/- 0.05 cavitation number.

Nuclei Measurements

The importance of the nuclei content in the water on cavitation inception and desinence has been reported by Arndt and Keller (1992), Fruman *et al.* (1991, 1992), Gindroz and Billet (1993). These investigators have demonstrated the strong influence the freestream nuclei distribution can have on the conditions for inception. Therefore, the water quality in this effort was carefully considered.

The nuclei content was measured with Cavitation Susceptibility Meter (CSM) model GEC Alsthom ACB CERG. The principals and operation of a CSM are described in Gindroz & Briançon-Majollet (1992). The water passing through the CSM was drawn at the height of the test section and upstream from the test, contraction, flow management, and first turning vanes sections. The CSM was located 1.8 m below the point where the water was drawn, and the water was returned to the lower leg of the channel. The CSM was used to determine the nuclei density with varying DO content, and to establish if the polymer itself had an effect in the nuclei inception process.

There are biases and uncertainties due to the CSM fluid volume sampling at the inlet (Oldenziel 1982) estimated to be a difference of approximately 10% in over the range nuclei sizes studied, and due to the acoustic detection system for the incepting nucleus. The repeatability of the measurements of the CSM for a given fluid was measured by taking three sets of data for the range considered in this effort. The log of each data set was line fit with R-square values of better than 0.98. The nuclei density for 8 different critical pressures were estimated with the linear best fit equation for the three data sets and the predicted values standard deviation and mean was computed. Based on these results it was found that the CSM was accurate within +/- 15% of the measured nuclei density for a given critical pressure. Therefore, the CSM would provide a good relative measure of the nuclei in the fluid under different DO content and polymer concentrations.

The nuclei content was measured for water that was used to fill the tunnel at the beginning of the experiments and then de-aerated to 25% DO with a vacuum pump system for approximately three hours. After de-aeration, tests were conducted for eight hours with the DO monitored, and then the water was drained. It was also measured for water that was de-aerated to 25% and then slowly aerated to 70% using the de-aeration system but under atmospheric pressure. The 70% DO water is similar to that injected for the cavitation study. In addition, the same 70% DO water used for the nuclei content measurement was mixed with 4000 *wppm* polymer solution to achieve 31 *wppm* and 125 *wppm* solutions used for nuclei content measurements.

Stereo Particle Imaging Velocimetry

Stereo Planar Particle Imaging Velocimetry (SPIV) was used to measure the vortical flow field in a plane downstream of the hydrofoil that was perpendicular to the flow direction. The location of the SPIV light sheet was 0.25, 0.5 and 1 chord-lengths downstream from the tip of the foil (Figure 3). A double-pulsed light sheet 6-7 mm thick was created perpendicular to the mean flow direction with two pulsed Nd:YAG lasers (Spectra Physics model Pro-250 Series), and three cylindrical lenses (60 mm, -150 mm and 200 mm focal length). Glass prisms were mounted to the side windows of the test-section for viewing the light sheet with reduced optical distortion. Double-pulsed images of the light sheet with a time lag of 25 microseconds were acquired with two digital cameras (LaVision FlowMaster 3S) capturing 4 images of 1280 x 1024 pixels, 35mm x 25mm. Two cameras with 105mm focal length macro Nikon lenses were used with Scheimpflug mounts to enable focusing of the plane of the light sheet. Optical distortion of the planar light-sheet images was corrected through a calibration procedure that employed the imaging of a regular grid (crosses at 4 mm intervals) placed on the same plane as the light sheet. The grid was immersed in water during calibration. The flow was seeded with silver coated glass spheres with an average diameter of 10 micron. Velocity vectors were produced from the double-pulsed images using the LaVision image analysis software DaVis® 7.2. Multi-interrogation processing (128 by 16 pixels) with a final window size of 16 by 16 pixels was used with 50% window overlap in the final pass to produce 179 by 129 in-plane velocity vectors at least 0.196 *mm* spacing. A series of 500 double-pulsed images are collected with a sampling rate that ensures that they are uncorrelated individual samples of the flow field. The 500 vector fields are averaged to produce the final flow field used to estimate the various flow parameters reported in this effort. The extent of vortex wandering was negligible (Baker *et al.,* 1974). The uncertainty in the in-plane velocity measurements is estimated to be +/- 3% while the out-of-plane component was estimated to be +/- 6%. The flow field was measured for a wide range of injected polymer solution concentrations and mass injection rates (Table 3).

RESULTS & DISCUSSION

Nuclei Measurements

The CSM can generate in the Venturi fluid tensions of a maximum of 10^2 kPa. Brennen (1995) relate the tension for a clean gas bubble nucleus to incept to its radius, R_n:

$$R_n > \frac{4S}{3(P_v - P_{CR})} \qquad (4)$$

where S is the surface tension and P_{CR} is the required critical pressure for the nucleus to incept, and this relationship is used to relate the critical tension in the throat of the CSM to the reported nuclei size. The CSM data were used to determine the most likely portion of the free-stream nuclei population that was activated during inception, to ensure that the nuclei populations were consistent over the course of the experiments, and to determine is the presence of polymer in the flow altered the susceptibility of the freestream nuclei population.

The results are plotted in Figure 4. A critical tension of 10^2 *kPa* corresponds to a 1 micron nucleus or greater, and a 10 *kPa* critical tension corresponds to a 10 micron nucleus or greater. There are at least 100 to 1000 times more 1 micron, nuclei than 10 micron nuclei, and very few 100 micron nuclei. It is also apparent that increasing the DO content from 25% to 70% increases the availability of nuclei in the range from 10 micron to 5 micron by an order of magnitude. The number of small nuclei, 1 micron, did not have a similar increase in density.

It was observed that the presence of polymer in the free-stream flow (a "polymer ocean") did not affect the critical pressure to inception for the nuclei. This result is in agreement with prior work from Chahine and Fruman (1979) who examined the formation of a spark generated bubble in polymer solution.

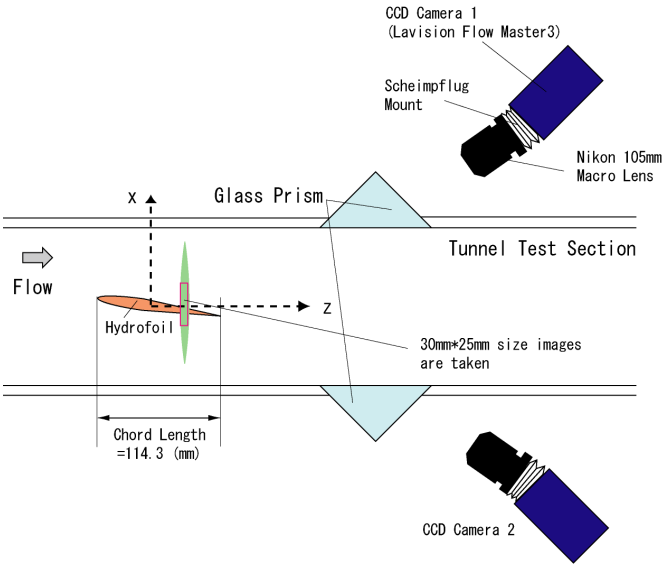

Figure 3: Stereo PIV set up: the laser sheet and imaging set up is fixed, the foil was mounted at 3.6 and 3.9 downstream from the tunnel test section inlet to respectively measure the flow field at z/c =50% and 25% downstream from the foil tip.

(a)

C (wppm) \ Q_{jet}	2.8 *cc/s*	5.6 *cc/s*	11.3 *cc/s*	22.6 *cc/s*
0	X		X	X
31	X	X	X	X
125	X	X	X	X
500	X		X	X

(b)

C (wppm) \ Q_{jet}	2.8 *cc/s*	5.6 *cc/s*	11.3 *cc/s*	22.6 *cc/s*
0	X		X	X
31	X	X	X	X
500	X	X	X	X

Table 3: flow conditions for the SPIV measurements. U_∞ = 8 *m/s*. (a) z/c = 0.25, (b) z/c = 0.5

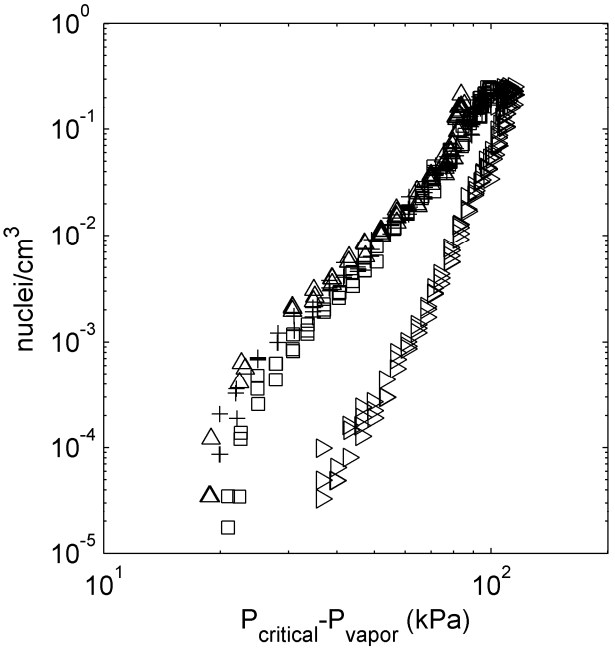

Figure 4: Nuclei distributions measured with the CSM: ☐ Water 70% DO; ▷ Water 25% DO; △ 31 wppm Polymer Ocean at 70% DO; + 125 wppm Polymer Ocean at 70% DO.

Average Flow Field of the Tip Vortex

SPIV measurements were used to determine the time-averaged properties of the primary tip vortex formed by the hydrofoil. Figure 5 shows two of the visualization planes that intersected the vortex downstream of the hydrofoil tip for U_∞ = 8 *m/s*. The local circulation, Γ, was estimated *via* a surface integration the in-plane vorticity field computes from the SPIV velocity data. An estimate of the total circulation was computed Γ using areas of increasing radius. It was found that at 1 chord length downstream of the circulation converged at a radius of 7.3 *mm* to a Γ = 0.12 +/- 0.01 m^2/s. At 0.25 and 0.5 chord-lengths, the wake of the hydrofoil prevents the estimation of circulation beyond 7.5 *mm* though vorticity was observed beyond that radius. It was found that the Γ was 0.10 +/- 0.01 m^2/s and 0.12 +/- 0.01 m^2/s at 0.25 and 0.5 chord-lengths, respectively.

The core radius, r_c, was estimated by determining the location of the maximum in-plane tangential velocity. The radii were measured to be 1.8 +/- 0.1 *mm*, 1.8 +/- 0.1 *mm* and 2.0 +/- 0.1 *mm* for 0.25, 0.5 and 1 chord lengths downstream from the tip. The mean axial velocity in the core of the vortex was also measured as 8.9 +/- 0.5 *m/s* for 0.25 and 0.5 chord lengths downstream, and 8.5 +/- 0.5 *m/s* at 1 chord length downstream, all for the baseline condition.

The circulation, core radius, and mean axial velocity of the core were determined for the cases listed in Table 3. In general, injection did not significantly modify the average flow fields. Instead, any differences detected were within the measurement uncertainty. The average pressure coefficient within the vortex core was computed using a method similar to that reported by Liu and Katz (2006). The static pressure was estimated by integrating Euler's equation in the vector field plane from a reference location at the edge of the SPIV plane to the vortex center. The estimate of the static pressure at the reference location at the edge of the image was obtained from a measure of the static pressure at the tunnel wall, P_∞. Then, Bernoulli's equation was used to estimate the pressure at the edge of the SPIV plane. The path of integration was varied from reference locations to the core, and the core static pressure, P_{core}, was taken as the average from the core pressure estimate computed for the different paths. The pressure coefficient, Cp, was defined as:

$$Cp = \frac{P_{core} - P_\infty}{\frac{1}{2}\rho U_\infty{}^2} \qquad (5)$$

Due to the presence of the foil in the SPIV image it is not possible to use all the possible paths from the edge of the SPIV image to the assumed vortex core center (where the tangential velocities minimize). Figure 6 shows an example of the SPIV averaged cross-stream velocity plane and the integration paths used to estimate the core pressure P_{core}.

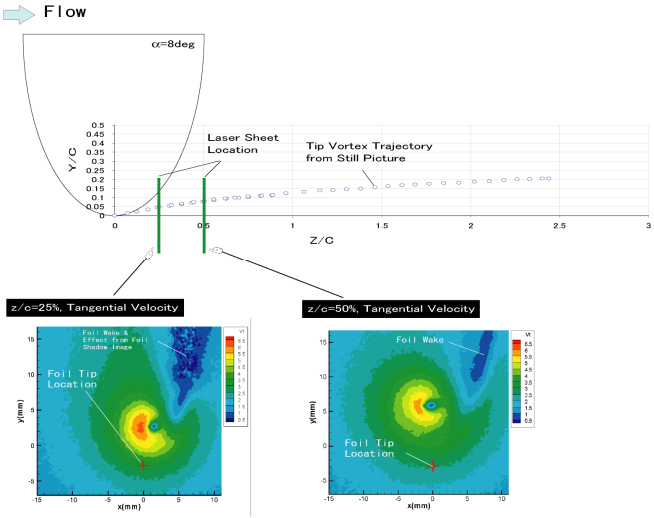

Figure 5: Average flow field measurement locations and vortex trajectory. Vortex trajectory was obtained from a still image picture of a fully cavitating TVC. The contours are the results obtained of the baseline at U_∞= 8 *m/s*, α = 8 degrees without injection.

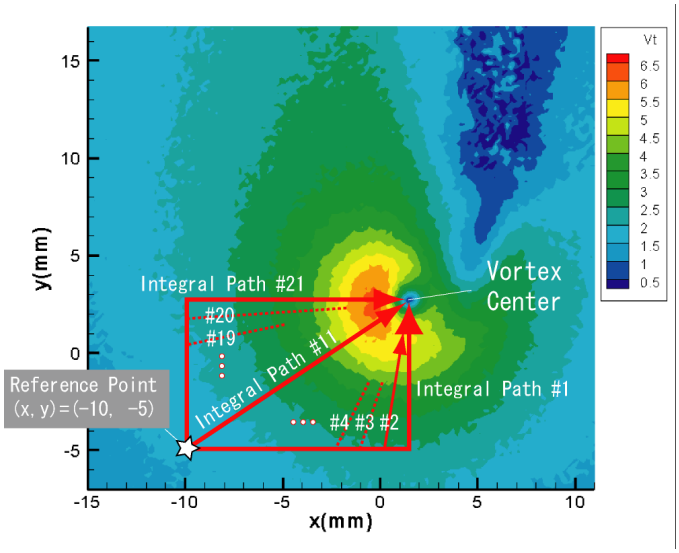

Figure 6: Integration paths used to estimate the average core pressure from the SPIV flow-field measurements.

The baseline values for -*Cp* were 2.3 +/- 0.2, 1.8 +/- 0.2 and 1.4 +/- 0.2 for 0.25, 0.5 and 1 chord lengths downstream from the tip of the hydrofoil. The *Cp* values were also computed for the conditions listed in Table 3. These results were then compared to the cavitation inception values measured in Yakushiji *et al.* (2008) for the baseline condition, as shown in Figure 7 and 8.

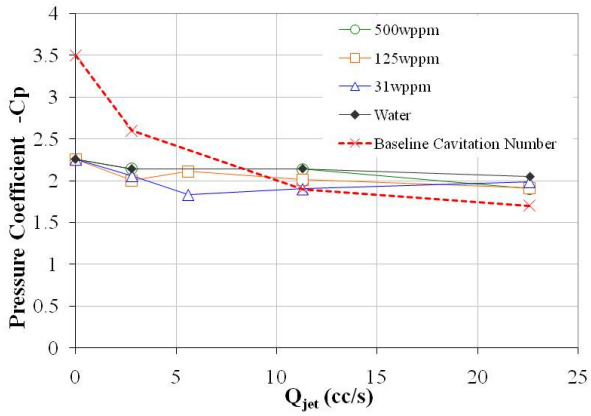

Figure 7: Estimated average static pressure at vortex center at *z/c* = 0.25. The Baseline Cavitation Number, σ_I, for TVC inception is without injection and U_∞ = 8 *m/s* from Yakushiji *et al* (2008).

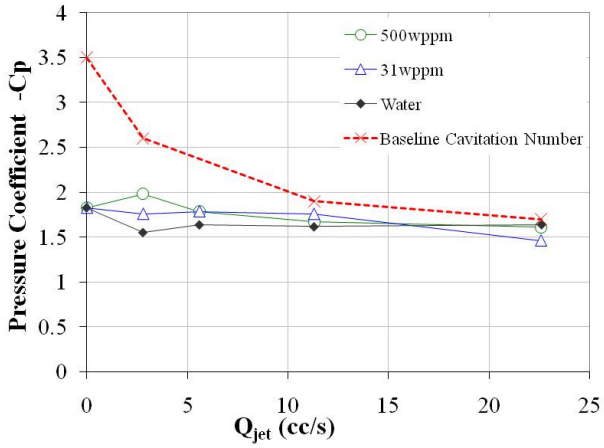

Figure 8: Estimated static pressure at vortex center at $z/c = 0.50$. The Baseline Cavitation Number, σ_I, is for TVC inception is shown was without injection at $U_\infty = 8$ *m/s* from Yakushiji *et al.* (2008).

Cavitation Inception and Desinence Without and With Injection

The effects of injecting water or a polymer solution were estimated for the experimental conditions listed in Table 2. The cavitation number for desinence ($B_{ratio} = 0.9$) and inception ($B_{ratio} = 0.01$) was observed for each condition. The desinence value was expected to correspond to the average minimum value of $-Cp$, and this was largely the case. The cavitation inception number is much more sensitive to the nuclei content and unsteady flow phenomenon, however. Arndt and Keller (1992) observed that the cavitation inception value was higher than the estimated $-Cp$ value from the flow and conjectured that this was due to turbulence in the vortex core. Similarly, Golapan *et al.* (1999), Iyer and Ceccio (2002), and Chang *et al.* (2007) related incipient vortex cavitation to localized, strong, and transient reduction in the fluid static pressure. Under these circumstances, inception will occur at cavitation numbers that are much higher than the average minimum value of vortex core pressure.

This was observed in the current investigation, as shown in Figures 7 and 8 for the non-injection conditions, where the baseline cavitation number for inception is substantially higher than the minimum average value of $-Cp$. However, the injection of water and polymer into the core of the vortex reduced the inception cavitation number to the minimum value of $-Cp$.

Figure 9 shows the cavitation inception and desinence number compared to the estimated Cp values for varying Q_{jet}/Q_{core}. The polymer flux is defined as $C\ Q_{jet}/Q_{core}$, where C is the concentration of the polymer. At zero polymer flux and injection rate (baseline), it is apparent that $-Cp$ matches the cavitation desinence number. But, the difference between the inception σ and $-Cp$ is of order unity. Hence, inception is occurring at a free-stream pressure that is significantly higher than would be expected simply from estimated the average minimum pressure in the TVC core.

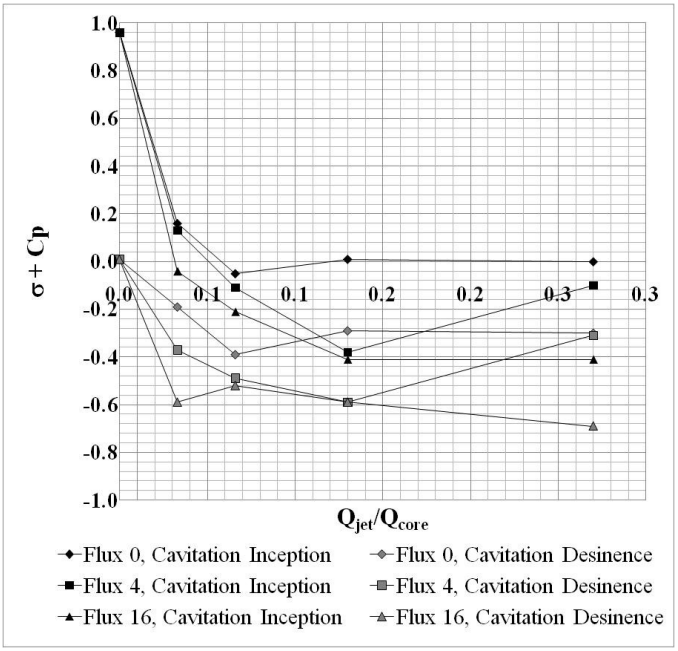

Figure 9: The influence of injection on $\sigma + Cp$. The experimentally observed inception and desinence cavitation numbers are used to plot $\sigma + Cp$ against injection rate Q_{jet}/Q_{core} for different levels of polymer flux $C\ Q_{jet}/Q_{core}$ for $U_\infty = 8$ *m/s*.

Figure 10 compare results form this study with some previously reported results. Fruman *et al.* (1995) reported that polymer injection lowers the cavitation number (either incipient or desinence) to a value similar to $-Cp$. For the data obtained by Yakushiji *et al.* (2008) the water injection was not sufficient to drop the cavitation number to $-Cp$. However, the preparation of the water to be injected in these experiments may have contained higher level of nuclei (compared to the solutions of polymer that were injected). In the present study, care was taken to match the nuclei content of all injectants.

Water is injection was examined for varying Q_{jet}/Q_{core}. Here, the polymer flux is zero since $C = 0$. The injection of water reduced both the inception and desinence cavitation number. With sufficiently high level of injection, $\sigma + Cp$ falls close to zero. The uncertainty in $\sigma + Cp$ is +/- 0.2 (largely due to the uncertainty in Cp). But, the drop in the inception value significantly exceeds the uncertainty. The injection of a polymer solution provided an additional drop in the cavitation number for both inception and desinence of ~ 0.2 to 0.4. At low concentrations the effect was not as consistent at higher Flux rates, probably due to polymer degradation as it was being injected.

Similarly, Figure 11 shows an overly of the data from this effort and others. The cavitation inception number resulting from water injection alone, σ_m, for a given volumetric flux, was subtracted from the value observed with the injection of polymer solutions at the same volume flux. It is apparent the polymer solution did provide some additional suppression for the 10 *m/s* data reported here and from the data of Fruman *et al.* (1995). It should be noted that Fruman *et al.* (1995) did not observe an effect of cavitation desinence when injecting water. This finding does not contradict the current study since

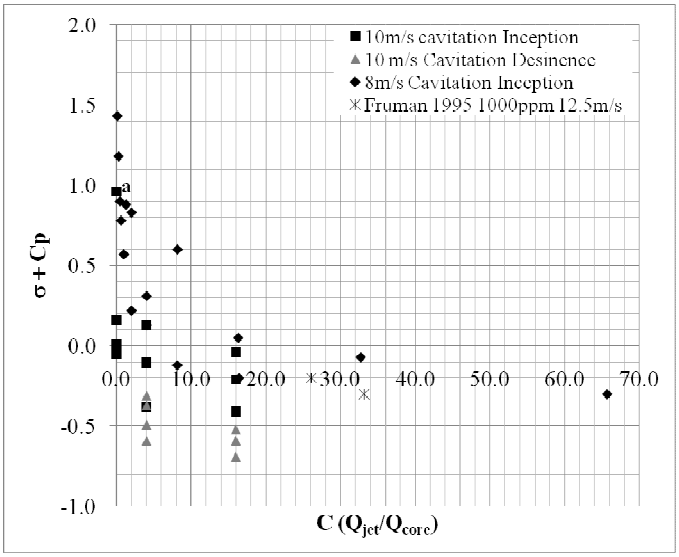

Figure 10: The influence of injection on $\sigma + Cp$ as a function of polymer flux, $C\ Q_{jet}/Q_{core}$. A delay in inception is observed for fluxes of water alone and polymer. As the flux increases, the effect saturates. The data for 8 *m/s* is from Yakushiji *et al.* (2008).

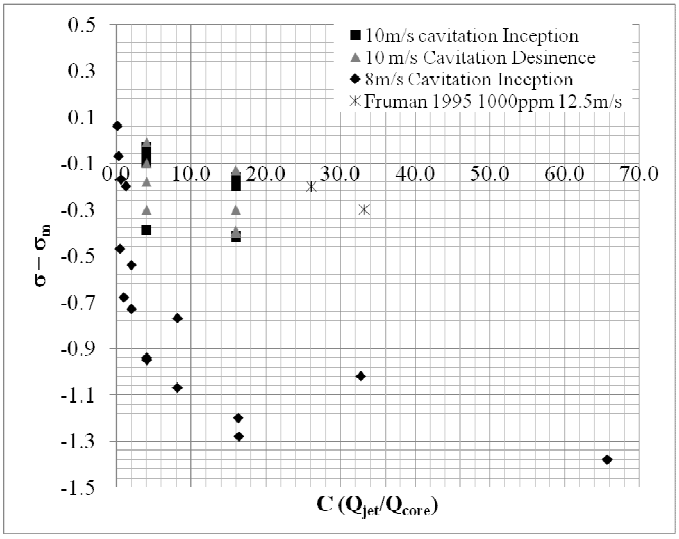

Figure 11: The difference between the inception or desinence cavitation number observed for water injection (σ_m) and injection with polymer solutions as a function of $C\ Q_{jet}/Q_{core}$. The additional suppressing effect of polymer less than 0.4 cavitation number for both Furman's and the current study (10*m/s*). The data for 8 *m/s* is from Yakushiji *et al.* (2008).

injection of water did not significantly change the desinence cavitation number here as well. It only affected the cavitation inception number. For the 8 *m/s* data set, as mention above, the authors suspect that the difference in the results were due to a variation in the nuclei content of the injectants. This reaffirms the important role that nuclei play in TVC inception and the care that must be taken to produce consistent and repeatable results.

Cavitation Inception Localization

The spatial location of cavitation was studied to potentially identify the location of minimum pressure in the vortical flow and any change that may occur when mass was injected to the core of the vortex. Table 4 shows a summary of the results. It was found that the average location of the events occurred at ~0.2 chord-lengths downstream from the hydrofoil tip, which coincides with the estimated location of lowest average core pressure of the vortex. There were cases while injecting mass where the average inception location was upstream from 0.2, and this was due to the presence of a small bubble in the injectant. There were also some incipient TVC bubbles observed relatively far downstream of x/c ~0.2, these were events that were due to nuclei capture, as discussed by Oweis *et al.* (2005). Given the relatively low event rates at inception, it is likely that only the largest nuclei are incepted by the vortex. This is also consistent with the observation that, inception takes place when $\sigma = -Cp$ for many cases with injection, implying that a near-zero tension is required for inception.

Sensitivity Analysis of the Core Pressure to the Vortex Properties

The above data show that mass injection did not change the average location of inception ($x/c \sim 0.2$). However, injection of both water and polymer solutions did reduced the cavitation inception number. The process of injection did not substantially alter the average flow of the vortex, as evidenced by the SPIV measurements. This suggests that the injection process may have altered the unsteady character of the vortical flow, especially in the region of the tip. However, since there is a finite uncertainty in the average flow-field measurements, it is important to understand how modest changes in the vortex characteristic might compound to produce a substantial change in the average core pressure. Choi and Ceccio (2007) report an equation to estimate Cp of the vortex core assuming that the vortex has a Gaussian velocity profile:

$$Cp = -\frac{\eta}{2}\left(\frac{\Gamma}{\pi r_c U_\infty}\right)^2 + \left(1 - \left(\frac{U_c}{U_\infty}\right)^2\right) \qquad (6)$$

Q_{jet}/Q_{core}	Polymer Flux CQ_{jet}/Q_{core}	σ	Inception σ_I	Event rate (1/*s*)	Events Observed	Events Observed $x/c > 0.5$	% Events Observed $x/c > 0.5$	Average Location (x/c)	Stan. Dev. Location (x/c)	Ave. Loc. $x/c < 0.5$ (x/c)
No Injection	0	3.3	3.3	1 or less	20	0	0%	0.21	0.14	0.21
No Injection	0	2.3	3.3	5.4	17	1	6%	0.18	0.29	0.11
No Injection	0	2.5	3.3	5.7	18	0	0%	0.12	0.06	0.12
No Injection	0	3.3	3.3	1 or less	20	0	0%	0.21	0.14	0.21
0.033	0	2.5	2.5	2.8	31	12	39%	0.33	0.38	0.07
0.033	0	2.7	2.5	1.6	31	4	13%	0.29	0.32	0.16
0.033	0	2.9	2.5	1.4	27	1	4%	0.23	0.22	0.20
0.13	0	2.1	2.3	3.2	35	13	37%	0.45	0.39	0.19
0.13	0	2.3	2.3	3.3	21	5	24%	0.35	0.23	0.24
0.13	0	2.5	2.3	2.1	15	1	7%	0.26	0.22	0.23
0.27	0	2.6	2.3	28	88	75	85%	0.74	0.26	0.44
0.033	4	2.4	2.4	18.8	74	15	20%	0.31	0.44	0.1
0.066	4	2.3	2.2	2.55	2	0	0%	0.19	0.22	0.19
0.13	4	1.8	1.9	5.4	142	102	72%	0.83	0.48	0.21
0.27	4	2.1	2.2	7.5	41	5	12%	0.13	0.31	0.02
0.033	16	2.4	2.3	20	47	11	23%	0.33	0.32	0.17
0.066	16	2.0	2.1	7.6	12	8	67%	0.63	0.4	0.18
0.13	16	1.6	1.9	12.4	39	34	87%	0.93	0.41	0.31
0.27	16	1.6	1.9	28	69	1	1%	0.05	0.15	0.03

Table 4: The event rates and location of incipient TVC bubbles measured for varying injection rates and polymer fluxes. The location of inception is ~ 0.2 *x/c*. However, some nuclei were captured by the vortex and incepted at a location $x/c > 0.5$ for all conditions, and there were some cases of TVC inception due to the introduction of bubbles through the injector.

where $\eta = 0.87$, $\beta = 0.715$, Γ is the circulation, r_c is the core radius, and U_c is the core axial velocity. At 0.25 chord-lengths downstream from the tip the vortex is not completely rolled up. Nonetheless, the *Cp* value predicted using Equation 6 for the Γ = 0.1 m^2/s and r_c = 1.8 mm (as measured with SPIV) was -2.3, the same value estimated *via* the integral of Euler's equation in the SPIV measured velocity plane discussed above.

Using Equation 6, the sensitivity of *Cp* to the core radius and the core axial velocity can be estimated for the vortex studied here. Specifically, an increase in core radius by ~10% creates an increase in *Cp* by ~15% and a decrease in core radius by ~10% creates a drop *Cp* by ~20%. Changes in the core axial velocity by +/- 10% will cause a proportional change in *Cp* by approximate -/+10%. A change in circulation by +/-10% causes a change in *Cp* by -/+20%. Variation in circulation produces the largest change in *Cp*. A +/-3% variation in free-steam velocity results in a *Cp* variation of -/+ 6%.

For the baseline case, inception occurred at σ = 3.3, or a value ~50% higher than the value derived from the averaged flow field. Assuming a constant circulation, the average axial velocity of the vortex would have to grow to $1.5U_\infty$. Or, the core radius would have to shrink by 20%. Baker *et al* (1974) observes a 5-10% wake in the core and peak fluctuations of 2.5% in the core velocity at 10 and 20 chord-lengths. Green and Acosta (1991) took measurements at 2 chord-lengths downstream from the tip of a NACA 66 and observed that there can be an axial velocity of 1.6 U_∞ with fluctuation of r.m.s of 0.2. Similarly, Fruman *et al.* (1992) report that axial jets of the order of 30% to 60% the freestream velocity were observed in the tip region of an elliptical hydrofoil. It is also reported that the r.m.s fluctuations increased with increasing Reynolds number.

The case of cavitation desinence the average flow field should suffice to provide an indication of the source of the decrease in $-Cp$. Based on Equation 6, a change in the core radius of +8% would provide the measured change in *Cp*. This corresponds to a +0.1 mm change. At the highest flux rate (16 *wppm/s*) the r_c measured was 1.9 mm which is sufficient to provide the requisite increase in *Cp* of 0.3. These are measurable changes in the average flow field. However, such systematic changes in the average vortex properties were not observed using the SPIV data.

CONCLUSION

In the present study, the injection of water and polymer solution have been shown to suppress the inception of tip vortex cavitation. Mass injection delayed inception of TVC inception until it reached the desinence value. Moreover, TVC desinence was delayed by 0.2 to 0.5 cavitation number from the baseline (non injection) value through mass injection of an aqueous polymer solution.

The mechanism which provides the suppression effect was shown to be different for cavitation inception and desinence. In the case of desinence, the measured changes in the average vortex properties (and, hence, the average minimum pressure in the vortex) with and without injection were consistent with the observed changes in the desinence cavitation number. However, the significant suppression of TVC inception with injection could not be related to the modest changes in the averaged flow field due to mass injection.

Therefore, the expected cause of the TVC inception delay is most likely due to a change in the *unsteady* tip flow. In the next phase of our study, we will use Laser Doppler Velocimetry

(LDV) to characterize the change in the unsteady flow in the region of TVC inception. Unlike the SPIV measurements, which are quite spatially filtered, LDV measurements focused on the inception location may provide insights into strong variation in the vortex maximum tangential velocity, axial flow speed, and magnitude of turbulent fluctuations in the core.

The possibility exists that the unsteady component of the flow could produce large tensions that could lead to the inception of smaller nuclei. However, it is likely that the largest nuclei were incepted, as little tension was needed to produce TVC, such that $\sigma_i >= -Cp$ for these flows. This would reduce the nuclei scale effect, at least for flow with relatively abundant nuclei.

More interestingly, it is unclear what flow underlying mechanism produces the unsteady flow phenomena that lead to inception under the baseline (non-injection) conditions. As stated above, researchers have postulated a number of different possible flow mechanisms. It the unsteadiness is associated with variation of the properties of the primary tip vortex, then scaling methods used to predict the strength, core size, and axial jetting, and core turbulence level of the primary vortex may ultimately be useful with respect to scaling. It is also possible that the dynamics of smaller scale, secondary vorticity in the tip region may be important and the vortex rolls-up, and these dynamics would be harder to capture with traditional scaling methods.

Therefore, our future objective is to investigate the underlying cause of flow unsteadiness and inception for the baseline flow, and to determine how mass injection may reduce, disrupt, or modify the tip flow. The data presented here indicate that the water injection alone may be sufficient to disrupt the tip flow. It is unclear is the added viscoelasticity of the injected polymer solutions lead to a separate mechanism of flow perturbation.

Finally, it is important to point out the relatively low Reynolds numbers of this (and other) investigations reporting TVC suppression with mass injection, as compared to prototype scale. Examine of the flow at higher Reynolds number may be necessary to permit higher fidelity measurement of the tip flow region, and to determine if the TVC suppression observed here is a scalable phenomenon.

ACKNOWLEDGMENTS

This work was supported by the Office of Naval Research under grant number N00014-07-1-0471, Dr. Ki-Han Kim program monitor, and the National Science Foundation through the Michigan Alliance for Graduate Education and the Professoriate.

REFERENCES

Green, S.I. & Acosta, A.J. "Unsteady flow in trailing vortices", J. of Fluid Mech., vol. 227 , 1991, 107 - 134

Arndt, R.E.A., "Cavitation in vortical flow", Annu. Rev. Fluid Mech. 34, 2002, pp 143–175.

Arndt, R.E.A. and Keller, A., "Water quality effects on cavitation inception in a trailing vortex", Transactions of the ASME – Journal of Fluids Engineering, Vol. 114, Sept. 1992.

Arndt, R.E.A. and Maines, B.H., "Further studies of tip vortex cavitation", The Second International Symposium on Cavitation, April 1994, Tokyo, Japan

Arndt, R.E.A. and Maines, B.H., "Nucleation and bubble dynamics in vertical flows", Transactions of ASME Journal of Fluids Eng., Vol. 122, Sept. 2000, pp 488-493

Baker, G.R., Barker, S.J., Bofah, K.K. and Saffman, P.G. "Laser anemometer measurements of trailing vortices in water", J. of Fluid Mech., vol. 65, 1974, pp 325-336

Brennen, C.E. Cavitation and bubble dynamic. Oxford University Press, New York, 1995, pp 65-91

Chahine G. L., Frederick, G. F., Bateman, R. D., "Propeller tip vortex cavitation suppression using selective polymer injection", Journal of Fluids engineering, Vol. 115, 1993, pp 497-503

Chahine, G.L. and Fruman, D.H., "Dilute polymer effects on bubble growth and collapse", Physics of Fluids, Vol 22(7), July 1979, pp1406-1407

Choi, J. and Ceccio, S.L., "Dynamics and noise emission of vortex cavitation bubbles", Journal of Fluid Mechanics, Vol. 575, 2007, pp 1-26

Chang, N.A., Choi, J., Yakushiji, R., Dowling, D.R. and Ceccio, S.L., "Dynamics and noise emission of cavitation bubbles in multiple vortex flow", 6th International Conference on Multiphase Flow, ICMF 2007, Leipzig, Germany, July 9 – 13, 2007

Fruman, D.H. and Galivel, P., "Near-field viscoelastic effects during thin-slit drag-reducing polymer ejection", Journal of Rheology, Vol. 25(5), 1980, pp 627-646

Fruman, D.H., and Aflalo, S.S., "Tip vortex cavitation inhibition by drag-reducing polymer solutions", Journal of Fluids engineering, Vol. 111, June 1989, pp211-215

Fruman, D. H., Dugue, C., and Cerrutti, P. "Tip vortex roll-up and cavitation", Cavitation and Multiphase Flow Forum, ASME FED, Vol. 109, pp 43-48, 1991

Fruman, D. H., Dugue, C., Pauchet, A., Cerrutti, P., Brianson-Majollet, L., "Tip vortex roll-up and cavitation", 19th International Symposium on Naval Hydrodynamics, Seoul, Korea, August 1992

Fruman, D. H., Pichon, T., Cerrutti, P., 1995, "Effect of drag-reducing polymer solution ejection on tip vortex cavitation", Journal of marine science and technology, Vol. 1, 1995, pp13-23

Gindroz, B., and Billet, M. L., “Influence of the nuclei on the cavitation inception for different types of cavitation on ship propellers”, ASME FED, Vol. 177, Cavitation inception, Louisiana1993

Gindroz, B. and Briancon-Majollet, L., “Experimental Comparison between Different Techniques of Cavitation Nuclei Measurements”, Proc. 2nd International Symposium on Propeller and Cavitation, Hangzhou, China 1992

Gopalan, S., Katz, J. and Knio, O. “The flow structure in the near field of jets and its effect on cavitation inception”, J. Fluid Mech, Vol. 398, 1999, pp 1-43

Iyer, C.O. and Ceccio, S.L. “The Influence of Developed Cavitation on the Flow of a Turbulent Shear Layer” Phys. of Fluids, Vol. 14 (10), 2002, pp 3414–3431

Liu, X. and Katz, J., “Instantaneous pressure and material acceleration measurements using a four-exposure PIV system”, Experiments in Fluids, Vol. 41, 2006, pp227-240

Oldenziel, D.M. “A New Instrument in Cavitation Research: The Cavitation Susceptibility Meter” Journal of Fluid Engineering Vol. 136, 1982, pp136-142

Oweis, G., I. E. van der Hout, C. Iyer, G. Tryggvason, and S. L. Ceccio, "Capture and Inception of Bubbles Near Line Vortices," Physics of Fluids, Vol. 17, No. 2, Art. No. 022105, 2005

Souders W.G. and Platzer G. P., “Tip vortex cavitation characteristics and delay of inception on a three-dimensional hydrofoil”, 1979, DTNSRDC Technical Report 79/051

Souders W.G. and Platzer G. P., “Tip vortex cavitation characteristics and delay of inception on a three-dimensional hydrofoil”, 1981, DTNSRDC Technical Report 81/007

Ting, R.Y., “Cavitation Suppression by Polymer Additives: Concentration Effect and Implication on Drag Reduction”, AlChE Journal, Vol. 20, NO. 4, July 1974, pp 827-828

Virk, P.S. and Baher, H., “The effect of polymer concentration on drag reduction”, Chemical Engineering Science, Vol. 25, Jan. 1970, pp. 1183-1189

Winkel, E.S., Oweis, G.F., Vanapalli, S.A., Dowling, D.R., Perlin, M., Solomon M.J. and Ceccio S. L. “High-Reynolds-number turbulent boundary layer friction drag reduction from wall-injected polymer solutions”, Journal of Fluid Mechanics, Vol. 621, 2009, pp 259-288